INTERNATIONAL JOURNAL OF CURRENT RESEARCH IN CHEMISTRY AND PHARMACEUTICAL SCIENCES

(p-ISSN: 2348-5213: e-ISSN: 2348-5221)
www.ijcrcps.com

Research Article

GROWTH BEHAVIOR OF Fe DOPED MnO_2 NANOCRYSTALS FOR HIGH PERFORMANCE ELECTROCHEMICAL CAPACITOR

R. POONGUZHALI[1], N. SHANMUGAM[1], R. GOBI*[1] AND A. SENTHILKUMAR[2]

[1]Department of Physics, Annamalai University, Annamalai Nagar, Chidambaram 608 002, Tamilnadu, India.
[2]Environmental & Analytical Chemistry Division, School of Advanced Sciences, VIT University, Vellore, Tamilnadu, India

Corresponding Author: alankoffi007@yahoo.co.in

Abstract

In this work, the influence of Fe doping on the capacitive properties of MnO_2 was investigated. MnO_2 and $Mn_{1-x}Fe_xO$ (x=0.025, 0.05, 0.75, 0.1 and 0.125 M) nanocrystals are synthesized via chemical precipitation method. The structure and morphology of the products were characterized by X-ray diffraction (XRD), Fourier transform infrared spectroscopy (FTIR), and scanning electron microscope (SEM). The X-ray diffraction patterns reveal the tetragonal structure of the synthesized α-MnO_2 particles. Morphological studies exhibit the mostly spherical nature of the synthesized particles. The FTIR spectra confirm the presence of Mn−O bonds. The super capacitive properties of MnO_2 and MnO_2: Fe electrodes are investigated using cyclic voltammetry and choronopotentiometry. From the CV studies the super capacitance increases with low level of Fe incorporation (0.075 M), and achieved a maximum of 912 Fg^{-1} at a scan rate 10 mV s^{-1}.

Keywords: Nanocrystals, MnO_2, $Mn_{1-x}Fe_xO$, XRD, SEM and FTIR.

Introduction

Supercapacitors occupy a place between the batteries and conventional capacitors in the Ragone plot (energy density Vs power density). The batteries distribute high energy density and low power density, whereas, conventional capacitors deliver high power density and low energy density. This has triggered the need to develop the super capacitors as alternates to batteries and conventional capacitors (Nagamuthu *et al*., 2013). These supercapacitors have many potential applications such as power electronics, electric vehicles, computer backup, sensor and space flight technology (Rajendra Prasad and Miura, 2004). However, power and energy demands of these applications vary significantly (Conway, 1997; Conway, 1991). Depending on the charge storage mechanism supercapacitors are generally classified into two categories by the electric double layer capacitors (EDLCs) and Pseudocapacitors. The EDLCs exploit the electrostatic separation of charges at the electrode/electrolyte interface to improve the capacitance, which depends on the specific surface area of materials. However, the pseudo capacitors utilize fast and reversible surface or near surface reactions for charge storage (Wang *et al*., 2013; Jayalakshmi and Balasubramanian, 2008). The transition metal oxides like RuO_2, MnO_2, Co_3O_4, NiO, SnO_2, Fe_3O_4, V_2O_5, conducting polymers, and hybrid composites have best electrode materials for pseudcapacitors because of their variable oxidation states of metal ions which facilitate redox transitions and higher charge storage within the potential range of water decomposition (Sarkar *et al*., 2011; Zhang *et al*., 2011). These types of capacitors are under extensive investigation in the modern time because of high capacitance and high energy characteristics. Among the transition metal oxides, RuO_2 pseudo capacitors has been studied as highly suitable material with very good capacitive response (>1000Fg^{-1}). However, their high costs and toxic nature prevent their usage. Hence incredible efforts have been devoted to

searching for and developing alternative electrode materials with low cost, environmental friendliness, and enhanced performance, such as NiO, $Ni(OH)_2$, and MnO_2 are now quite active. MnO_2 is a significant and well studied material for supercapacitors (Yang *et al*., 2011; Kim *et al*., 2013; Li *et al*., 2011). The certain amount of elemental doping of a simple pseudo-capacitive metal oxides to form mixed metal oxides has been recognized to be an effective way to increase their specific capacitance, as confirmed by numerical studies such as Mn-Ni oxide, Mn-Co oxide and Mn-Fe, Ni-Ti oxide and ternary metal oxide system as Mn-Ni-Co, Co-Ni-Cu and Mn-Ni-Cu oxide etc. The mixed metal oxides have existence a multiple valance electrons, to activate a redox reaction with the electrolyte, so the specific capacitance increases in the transition metal oxides (Wen and Kang, 1998; Jayalakshmi *et al*., 2006). Among the systems, hematite systems have received careful attention due to their wide applications in oxygen electrode reactions. Both the MnO_2 and hematite (α-Fe_2O_3) have already been studied extensively because of their superior performance as the active electrode materials for the pseudocapacitors compared with the conventional carbon based materials. Moreover the low cost, good stability, non toxic and environmentally friendly nature of the MnO_2 and α-Fe_2O_3 coupled with their high redox activity make them suitable for the extensive application in pseudocapacitors (Patrice *et al*., 2004). In the present study, we have investigated the influence of the Fe doping on capacitor performance of MnO_2. The pristine MnO_2 and Fe doped MnO_2 samples were synthesized by precipitation processes. Further, the synthesized products were characterized by XRD, FT-IR, SEM and N_2 adsorption – desorption.

Materials and Methods

Chemicals

All chemical reagents were purchased in refined grade (E.Merck) and used without further purification. All the solutions were prepared in deionized water. Manganese acetate tetra hydrate [$C_4H_6MnO_4.4H_2O$], iron (III) nitrate nonohydrate [$Fe(NO_3)_3.9H_2O$] and potassium permanganate ($KMnO_4$) were used as precursors.

Synthesis of bare and Fe ions doped MnO_2 nanocrystals

For the synthesis of Fe doped MnO_2, 6.12 g (0.5 M) of manganese acetate tetra hydrate [$C_4H_6MnO_4.4H_2O$] was dissolved in 30 ml of deionized water was stirred vigorously by magnetic stirrer and iron (III) nitrate [$Fe(NO_3)_3.9H_2O$] of preferred mole was (0.00, 0.025, 0.05, 0.075, 0.1 and 0.125 M) prepared in 20 ml aqueous were mixed drop by drop. Then, 5.92 g (1 M) of potassium permanganate in 50 ml of deionized water was added drop by drop to the above mixture. The entire mixture was stirred vigorously using a magnetic stirrer. After 5 hrs of stirring a dark brown colored precipitate of precursor MnO_2 was obtained. The obtained precursor was washed alternately with deionized water and ethanol to remove the impurities. The washed products were dried in hot air oven at 80° C for 6 hrs to evaporate water and organic material to the maximum extent. Finally, the obtained product was annealed in a muffle furnace at 400° C for 3 hrs. The annealed powders were pulverized to fine powders using agate mortar for further characterizations. A similar method of preparation without the addition of Fe was used to synthesized undoped (bare) MnO_2 nanocrystals.

Material characterization

The crystalline phase and particle size of pure and Fe doped MnO_2 nanoparticles were analyzed by X-ray diffraction (XRD) measurement which was carried out at room temperature by using X'PERT-PRO diffractometer system (scan step of 0.05° (2θ), counting time of 10.16 s per data point) equipped with a Cu tube for generating Cu K_α radiation (k = 1.5406 Å); as an incident beam in the 2-theta mode over the range of 10°–80°, operated at 40 kV and 30 mA. The Fourier transform infrared (FTIR) spectra were carried out using SHIMADZU-8400 FTIR spectrometer in the range of 4000-400 cm^{-1}. The morphology of the product was observed by scanning electron microscopy (SEM; JEOL-JSM-56100) operating under 20 kV accelerating potential.

Electrochemical performance investigation

The electrochemical properties of the sample were investigated with cyclic voltammetry (CV), galvanostatic (GV) charge, discharge tests and Electrochemical impedance measurements carried out by using software –controlled conventional three electrode electrochemical cell (CHI660C electrochemical workstation), consisting of the glassy carbon electrode (GCE) was employed as the working electrode (WE), Ag/AgCl as the reference electrode, and the platinum wire as the counter electrode. The working electrode was coated with 0.5 µl of active material (MnO_2) dispersed in 2µl nafion solution. All the electrochemical measurements are performed in a 0.5 M KCl aqueous electrolyte solution at room temperature. The CV measurements were performed at different scan rate of 10, 20, 30, 40, 50, 70, 90 and 100 mVs^{-1}. GV charge- discharge measurements were conducted at various current densities of 10, 20, 30, 40, and 50 A g^{-1} for evaluating the specific capacitance, power density and energy density. A potential window in the range from -0.3 to 0.7 V was used in all the measurements.

Results and Discussion

Structural analysis

Fig.1 shows the X-ray diffraction (XRD) patterns of bare MnO_2 and different concentrations of Fe doped MnO_2 nanocrystals. The strong diffraction peak at 2θ = 37.20 °C matches with the α-MnO_2 according to a standard JCPDS file no: (44-0141). It confirms that, they obtained MnO_2 is main microcrystalline of α-MnO_2 (Zhang *et al*., 2013). All the diffraction peaks can be perfectly indexed to the tetragonal structure with an I4/m space group. The grain size was calculated by using the Scherrer's formula and estimated as 9.8 nm for pure MnO_2.

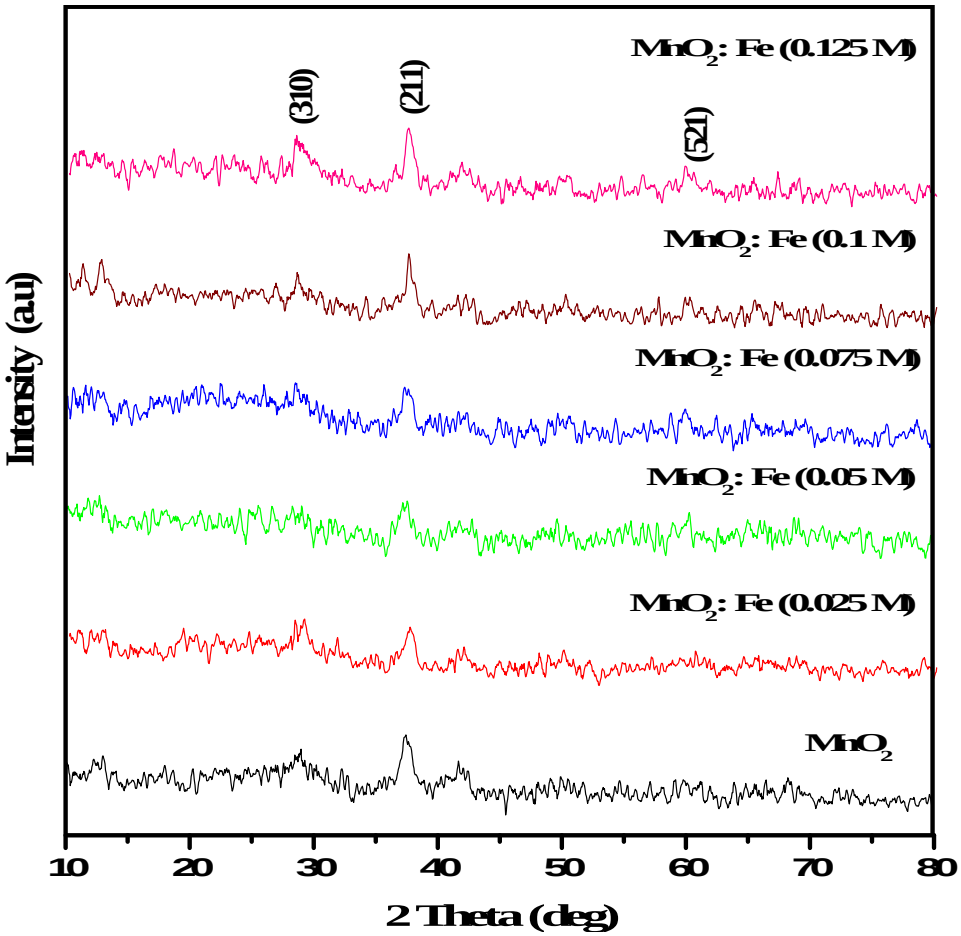

Fig. 1 X-ray diffraction patterns of pure and Fe-doped MnO_2 nanocrystals.

However, the estimated sizes for different concentrations (0.025, 0.05, 0.075, 0.1 and 0.125 M) of Fe doped MnO_2 samples are 4.1, 6.9, 8.36, 8.39 and 8.42 nm respectively. It also has been seen that the XRD peak intensity increases with increasing Mn content. There is no any extra peak of manganese metal oxide, or any impurity phases were observed. It indicates that all the samples are single phase. The Fe ions go to Mn site up to 0.125 M without changing tetragonal structure and no formation of secondary phases. The reflection peak in the diffraction patterns of Fe substituted MnO_2 nanocrystals are slightly shifted to lower angle as compared to the pure MnO_2 nanocrystals. It evidence that the Fe^{2+} ions go to Mn^{2+} ions.

Functional group analysis

In order to know the presence of functional groups in the synthesized samples, FT-IR spectra of undoped and different levels of Fe incorporated MnO_2 nanocrystals were recorded in the range of 4000-400 cm^{-1} and presented in Fig.2. The absorption bands around at 3439 cm^{-1} that could be observed in all the samples is due to the hydrogen - bonded hydroxyl groups, and several small absorption peaks at around 1000-1500 cm^{-1} are attributed to the bending vibration of O-H bonds. The absorption peak at 525 cm^{-1} can assign to Mn-O is bending vibrations; arise from MnO_6 octahedron vibration mode (Wu *et al*., 2012).

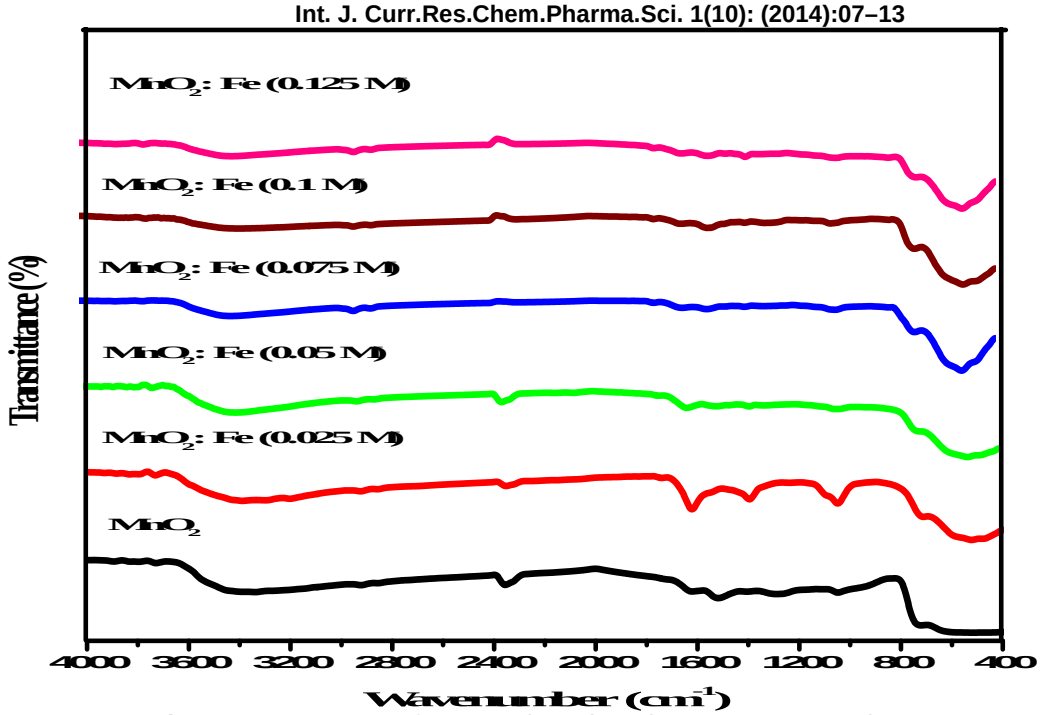

Fig. 2 FTIR patterns of pure and Fe-doped MnO_2 nanocrystals

Morphological analysis

The SEM micrographs of MnO_2 and Fe:MnO_2 (0.075 M) are presented in (Fig.3 (a, b)). From the micrographs of undoped MnO_2, it is observed that most of the particles are spherical in shape with sizes in the range from 20-30 nm. Most of the particles in the doped product are showing spherical morphology with sizes in the range of 15-30 nm. This indicates the effect of Fe doping on controlling the morphology of the MnO_2.

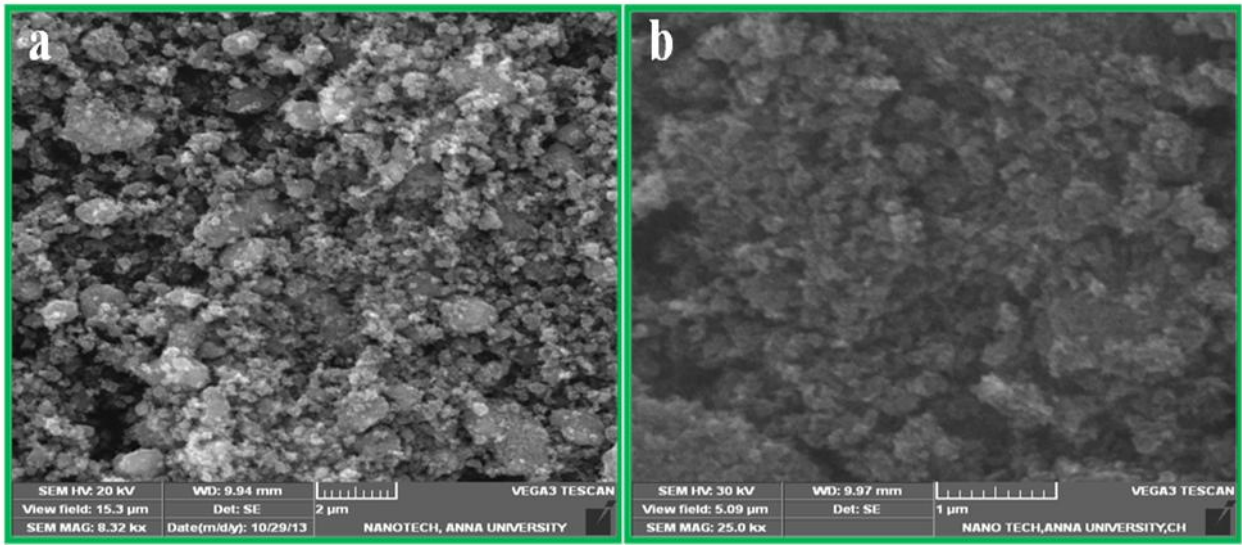

Fig. 3 (a, b) SEM images of pure and Fe-doped (0.075M) MnO_2 nanostructures

Electrochemical characterizations

The electrochemical performance of pure and Fe doped nanostructure electrode was evaluated using cyclic voltammetry and galvanostatic charge discharge studies. Fig 4 shows the typical CV curves of pure and Fe doped MnO_2 modified GCE electrode in a 0.5 M KCl aqueous electrolyte over the voltage range -0.3 to 0.7 V and at a constant scan rate 10 mVs^{-1}. All the curves show perturbed rectangular shape indicating the pseudocapacitance nature of the synthesized product. It has been found that the through introduction of Fe, the degree of change in the Mn oxidation state increases. In evaluation among the

samples MnO_2: Fe (0.075 M) shows the highest peak current density and the largest loop area representing the largest electrochemical capacitance (Shi *et al*., 2010). The specific capacitance of the electrode was calculated from the CVs according to the following equation (Dubal *et al*., 2012).

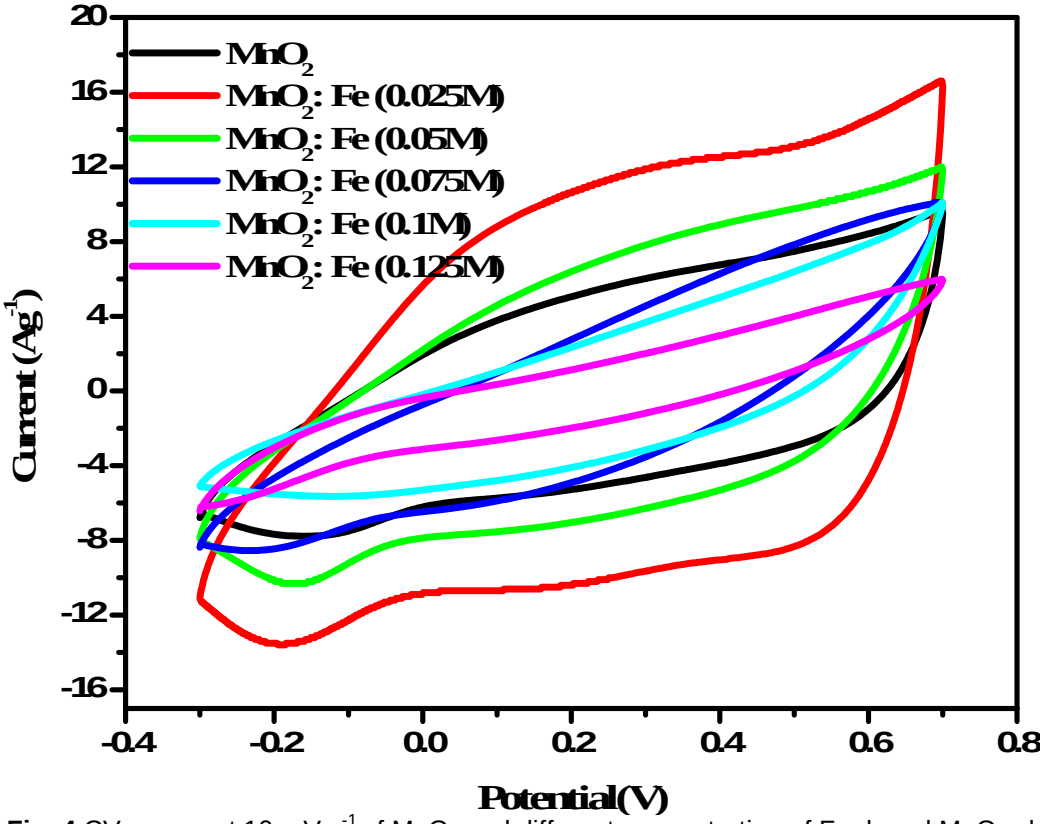

Fig. 4 CV curves at 10 mV s^{-1} of MnO_2 and different concentration of Fe doped MnO_2 electrodes

$$Cs = \frac{Q}{m\Delta v} \quad \ldots\ldots\ldots \quad (1)$$

Where Q is the average charge during anodic and cathodic scan, m is the mass of the active material (g), and Δv is the scan rate (mV s^{-1}). The calculated specific capacitance value of MnO_2: Fe (0.075 M) was higher than that of MnO_2, because the specific surface area of MnO_2: Fe was higher than that of MnO_2. However, the estimated specific capacitance values are 210, 620, 662, 912, 508 and 412 Fg^{-1} for pure and Fe doped MnO_2 at 0.025, 0.05, 0.075, 0.1 and 0.125 M respectively.

Effect of Fe doping concentration

Fig. 5 shows the variation in specific capacitance of prepared electrode versus the Fe content in the binary oxide. The data indicate that the specific capacitance of MnO_2 increase from 201 to 912 Fg^{-1} for MnO_2, Fe incorporated with MnO_2. However, further increasing 0.075 M of Fe content in the binary oxide the specific capacitance value decreased. This may be due to the decrease in the porosity of the MnO_2 electrode, which reduces the surface area of the electrode (Si Xu Deng *et al*., 2013). Our results indicate that using suitable Fe doped MnO_2 nanocrystals as electrodes can enhance the specific capacitance. The nanostructure composite material reduces the ion diffusion paths and provides more paths for electron conduction. The electrochemical activation of electrodes are calculated from the following equation (Liu *et al*., 2012).

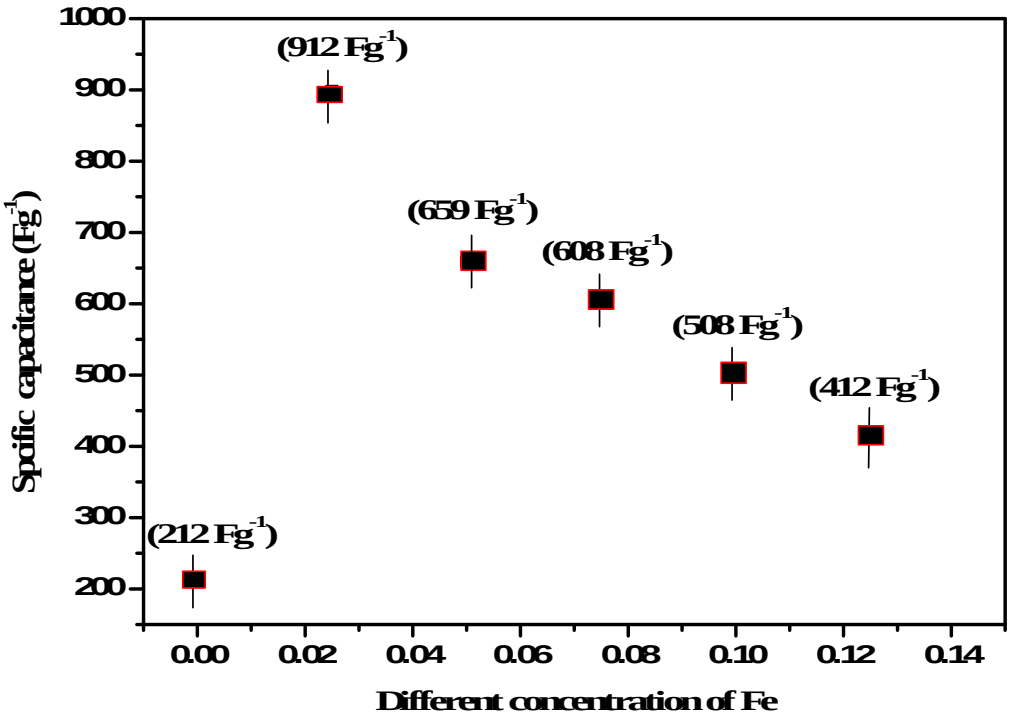

Fig. 5 The value of specific capacitance at different scan rate.of MnO_2 and different concentration of Fe doped MnO_2 electrodes

$$Z = C\Delta V \frac{M}{F}$$

Where C is the specific capacitance value (F g^{-1}) at 10mV s^{-1}, ΔV is the potential window, M is the molecular weight of MnO_2 (86.94 g), and F is the Faradic constant. The calculated Z values of pure MnO_2 and MnO_2: Fe composite materials are 0.18, 0.55, 0.59, 0.82, 0.32, and 0.19 respectively. The maximum Z value obtained for MnO_2: Fe (0.075 M), and the value is 0.82, it could be observed that about 19% electroactive sites are involved in the redox processes and also given a high specific capacitance (912 Fg^{-1}).

Conclusion

MnO_2 and different concentrations of Fe doped MnO_2 nanocrystals were synthesized through chemical precipitation method. The XRD results of the MnO_2 and Fe doped MnO_2 are poorly crystalline nature and showed tetragonal structure of the α-MnO_2 nanocrystals. The super capacitive properties of MnO_2 and MnO_2: Fe electrodes are investigated using cyclic voltammetry and choronopotentiometry. From the CV studies the super capacitance increases with low level of Fe incorporation (0.075 M), and achieved a maximum of 912 Fg^{-1} at a scan rate 10 mV s^{-1}.

References

Nagamuthu, S., S. Vijayakumar, and G. Muralidharan, Synthesis of Mn_3O_4/Amorphous Carbon Nanoparticles as Electrode Material for High Performance Supercapacitor Applications, Energy Fuels 27 (2013) 3508.

Rajendra Prasad, K., N. Miura, Electrochemically synthesized MnO_2-based mixed oxides for high performance redox supercapacitors, Electrochemistry Communications 6 (2004) 1004.

Conway, B. E. Electrochemical Supercapacitor, Scientific Fundamentals and technological Applications, Kluwer Accademic / plenum Pulishers. New York.1997.

B.E.Conway, Transition from “Supercapacitor” to “Battery” Behavior in Electrochemical Energy Storage, J. Eletrichem. Soc 138 (1991) 1539.

Wang, B., P. Guo, H. Bi, Q. Li, G. Zhang, R. Wang, J. Liu, and X. S. Zhao., Electrocapacitive Properties of $MnFe_2O_4$ Electrodes in Aqueous $LiNO_3$ Electrolyte with Surfactants, Int. J. Electrochem. Sci 8 (2013) 8966.

Jayalakshmi, M and K. Balasubramanian, Simple Capacitors to Supercapacitors - An Overview, Int. J. Electrochem. Soc 3 (2008) 1196.

Sarkar, D., G. Gopal Khan, K. Singh, and K. Mandal., High-Performance Pseudocapacitor Electrodes Based on α-Fe_2O_3/MnO_2 Core−Shell Nanowire Heterostructure Arrays, J. Phys. Chem. C 117 (2013) 1552.

Zhang, Y., G. Li, Y. Lu, L. Wan, Ai-Qin Zhang, Yan-Hua Song, Bei-li Huang, Electrochemical investigation of MnO_2 electrode material for super capacitors, International Journal of Hydrogen Energy 36 (2011) 11760.

Yang, Y., E. Liu., L. Li, Z. Huang, H. Jie Shen, X. Xiang, Nanostructured amorphous MnO_2 prepared by reaction of $KMnO_4$ with triethanolamine, Journal of Alloys and Compounds 505 (2010) 555.

Kim, M., Y. Hwang, J. Kim, Graphene/MnO_2-based composites reduced via different chemical agents for supercapacitors. Journal of Power Sources 239 (2013) 225-233.

Li, Y., H. Xie, J. Wang, L. Chen, Preparation and electrochemical performances of α-MnO_2 nanorod for supercapacitor, Materials Letters 65 (2011) 403.

Wen, T.C., H.M. Kang, Co-Ni-Cu ternary spinel oxide-coated electrodes for oxygen evolution in alkaline solution, Eletrochem. Acta 43(1998) 1729-1745.

Jayalakshmi, M., N. Venugopal, K. Phani Raja, M. Mohan Rao, Nano SnO_2-Al_2O_3 mixed oxide and SnO_2-Al_2O_3-carbon composite oxides as new and novel electrodes for supercapacitor applications, Journal of Power Sources 158 (2006) 1538.

Patrice, R., L. Dupont, L. Aldon, J.C. Jumas, E. Wang, J.M. Tarascon, Structural and electrochemical properties of newly synthesized Fe-substituted MnO_2 samples, Chem. Mater 16 (2004) 2772.

Xu, J., L. Li, W. Gou, α-Fe_2O_3 Nanotubes in Gas Sensor and Lithium-Ion Battery Applications. Adv. Mater 17 (2005) 582.

Zhang, H., Y. Wang, C. Wang, Influence of surfactant on the capacitive performance of manganese dioxide prepared at different temperatures, Energy Conversion and management 74 (2013) 286.

Wu, C., J. Ma, C. Lu, Synthesis and characterization of nickel–manganese oxide via the hydrothermal route for electrochemical capacitors, Current Applied Physics 12 (2012) 1190.

Shi, X., W. Zhu, J. Zaho, W. Ma, J. Mahaisalkar, S. Maria, T.L. Yang, Y. Zhang, H. Hang, H. Yan, Synthesis of porous NiO nanocrystals with controllable surface area and their application as supercapacitor electrodes, Nano Res 3 (2010) 643.

Dubal, D. P., W.B. Kim, C.D. Lokhande., Galvanostatically deposited Fe: MnO_2 electrodes for supercapacitor application, Journal of Physics and Chemistry of Solids 73 (2012) 18.

Wu, T., J. Li, L. Hou, C. Yuan, L. Yang, X. Zhang, Uniform urchin-like nickel cobaltite microspherical superstructures constructed by one-dimension nanowires and their application for electrochemical capacitors, Electrochimica Acta 81 (2012) 172.

Si Xu Deng, Dan Sun, Chun Hui Wu, Hao Wang, Jing Bing Liu, Yu Xiu Sun, Hui Yan., Synthesis and electrochemical properties of MnO_2 nanorods/graphene composites for supercapacitor applications, Electrochimica Acta 111 (2013) 707.

Liu, J., L. Fan, X. Qu., Low temperature hydrothermal synthesis of nano-sized manganese oxide for supercapacitors, Electrochimica Acta 66 (2012) 302.

